Eur J Neurosci. Author manuscript; available in PMC 2016 May 19.

Published in final edited form as:

Eur J Neurosci. 2009 March ; 29(5): 911–920. doi:10.1111/j.1460-9568.2009.06672.x.

Synchronous $GABA_A$-receptor-dependent potentials in limbic areas of the *in-vitro* isolated adult guinea pig brain

Laura Uva[1], **Massimo Avoli**[2,3], and **Marco de Curtis**[1]

[1]Unit of Experimental Neurophysiology and Epileptology, Fondazione Istituto Neurologico Carlo Besta, via Celoria 11, 20133 Milan, Italy

[2]Montreal Neurological Institute and Department of Neurology and Neurosurgery, McGill University, Montréal, QC, Canada

[3]Dipartimento di Medicina Sperimentale, Sapienza Universitá di Roma, Rome, Italy

Abstract

Epileptiform discharges are known to reflect the hypersynchronous glutamatergic activation of cortical neurons. However, experimental evidence has revealed that epileptiform synchronization is also contributed to by population events mediated by $GABA_A$ receptors. Here, we analysed the spatial distribution of $GABA_A$-receptor-dependent interictal events in the hippocampal/parahippocampal region of the adult guinea pig brain isolated *in vitro*. We found that arterial perfusion of this preparation with 4-aminopyridine caused the appearance of glutamatergic-independent interictal potentials that were reversibly abolished by $GABA_A$ receptor antagonism. Laminar profiles and current source density analysis performed in different limbic areas demonstrated that these $GABA_A$-receptor-mediated events were independently generated in different areas of the hippocampal / parahippocampal formation (most often in the medial entorhinal cortex) and propagated between interconnected limbic structures of both hemispheres. Finally, intracellular recordings from principal neurons of the medial entorhinal cortex demonstrated that the GABAergic field potential correlated to inhibitory postsynaptic potentials (membrane potential reversal, −68.12 ± 8.01 mV, $n = 5$) that were interrupted by ectopic spiking. Our findings demonstrate that, in an acute seizure model developed in the adult guinea pig brain, hypersynchronous $GABA_A$-receptor-mediated interictal events are generated from independent sources and propagate within limbic cortices in the absence of excitatory synaptic transmission. As spared or enhanced inhibition was reported in models of epilepsy, our data may support a role of GABA-mediated signaling in ictogenesis and epileptogenesis.

Keywords

epilepsy; $GABA_A$ receptors; interictal spikes; *in-vitro* isolated brain; parahippocampal cortex; piriform cortex

Correspondence: Dr M. de Curtis, as above., decurtis@istituto-besta.it.

Introduction

Epileptiform discharges in limbic cortices result from the synchronization of cortical neuronal networks sustained by glutamatergic mechanisms (Avoli *et al.*, 2002). Increasing evidence, however, supports the concept that inhibitory population events caused by the activation of $GABA_A$ receptors contribute to the synchronization of principal neurons during epileptiform interictal events and at the onset of a seizure (Avoli *et al.*, 1996, 2002; Köhling *et al.*, 2000; Gnatkovsky *et al.*, 2008; Bender *et al.*, 2007). Synchronous GABAergic potentials have been recorded in cortical slices maintained *in vitro* in a condition of enhanced excitability caused by application of the potassium channel blocker 4-aminopyridine (4AP) in the bathing medium (Aram *et al.*, 1991; Michelson & Wong, 1991; Perrault & Avoli, 1992). These potentials [which contribute to interictal spiking and ictogenesis in some *in-vitro* models of epileptic seizures (Avoli *et al.*, 2002)] are mirrored by synchronous depolarizations that are resistant to the application of *N*-methyl-D-aspartate (NMDA) and non-NMDA receptor glutamatergic antagonists, and are abolished by $GABA_A$ receptor antagonists (Perreault & Avoli, 1991; Michelson & Wong, 1994). $GABA_A$-receptor-mediated interictal potentials have been observed in several areas of the hippocampus proper (Michelson & Wong, 1991, 1994; Avoli *et al.*, 1996), in the entorhinal cortex (EC) and perirhinal cortex (Lopantsev & Avoli, 1998), and in the insular cortex (Sudbury & Avoli, 2007). Similar synchronous GABAergic potentials have also been identified in postsurgical cortical tissue obtained from patients suffering from drug-resistant epilepsy due to Taylor's type focal cortical dysplasia (Avoli *et al.*, 1994; D'Antuono *et al.*, 2004) and temporal lobe epilepsy (Kohling *et al.*, 1998; Louvel *et al.*, 2001; Cohen *et al.*, 2002; Huberfeld *et al.*, 2007). Moreover, inhibition was spared in early phases of temporal lobe epileptogenesis (Du *et al.*, 1995; Eid *et al.*, 1999) and was found to be enhanced in other models of epilepsy (Klaassen *et al.*, 2006), thus suggesting a potential role of enhanced GABA-mediated synchronization in epileptogenesis.

One important feature of these $GABA_A$-receptor-mediated events is their ability to propagate at a distance during excitatory transmission blockade. This characteristic propagation has been seen between different subfields of isolated hippocampal slices (Perrault & Avoli, 1992), in human neocortical tissue slices (Avoli *et al.*, 1994), and in extended EC / hippocampal rat slices (Avoli *et al.*, 1996). Several mechanisms have been proposed for such propagation including the spatial redistribution of extracellular potassium that transiently increases during each glutamatergic-independent potential (Avoli *et al.*, 1996; Morris *et al.*, 1996). Here we test the hypothesis that similar $GABA_A$-receptor-mediated interictal potentials propagate in a seizure model developed in the intact *in-vitro* whole-brain preparation (Llinas *et al.*, 1981; de Curtis *et al.*, 1991, 1998; Muhlethaler *et al.*, 1993). In this model long-range connections between brain structures, interhemispheric propagation and the extracellular milieu are functionally preserved (Biella & de Curtis, 2000; Biella *et al.*, 2001, 2002).

Materials and methods

Brains of adult Hartley guinea pigs (150–200 g) were isolated and maintained *in vitro* according to the standard procedure (de Curtis *et al.*, 1991, 1998; Muhlethaler *et al.*, 1993).

Briefly, the animals were anesthetized with sodium thiopental (125 mg / kg i.p., Farmotal, Pharmacia, Milan, Italy) and transcardially perfused with a cold (10°C) carboxygenated (95% O_2, 5% CO_2) saline solution (composition: 126 mM NaCl, 3 mM KCl, 1.2 mM KH_2PO_4, 1.3 mM $MgSO_4$, 2.4 mM $CaCl_2$, 26 mM $NaHCO_3$, 15 mM glucose, 2.1 mM HEPES and 3% dextran M.W. 70 000, pH 7.1). Following decapitation, brains were dissected out and transferred into the recording chamber. A cannula was inserted into the basilar artery and brain perfusion was restored at 6 mL / min with the above solution (15°C, pH 7.3) via a peristaltic pump (Minipulse 3, Gilson, France). The temperature of both the chamber and the perfusate was slowly raised to 32°C to perform electrophysiological recordings, and to maintain an anesthetized condition (Pearcy & Virtue, 1960). The number of animals used was minimized according to the international guidelines on ethical use of animals (European Communities Council Directive of 24 November 1986 (86 / 109 / EEC)). The experimental protocol was reviewed and approved by the Committee on Animal Care and Use and by the Ethics Committee of the Fondazione Istituto Neurologico.

Extracellular recordings were simultaneously performed in the piriform cortex (PC), the medial EC (m-EC) and lateral EC (l-EC), and different subfields of the hippocampus with both NaCl-filled micropipettes (5–8 μm tip diameter, 5–10 MΩ resistance) and 16-channel silicon probes that featured 16 recording sites separated by 50–100 μm on a single vertical shaft (NeuroNexus Technologies, Ann Arbor, MI, USA). In most experiments, recordings were obtained from both hemispheres. Intracellular recordings from the m-EC were performed with micropipettes filled with 2 M K-acetate. Signals were amplified using either a multichannel differential amplifier (Biomedical Engineering, Thornwood, NY, USA) or an intracellular amplifier (Neuro Data Instruments, New York, NY, USA). Data were digitized via an AT-MIO-64E3 National A / D Board (National Instrument, Milan, Italy) and analysed with custom-made software (ELPHO©) developed in Labview by Dr V. Gnatkovsky (Department of Experimental Neurophysiology and Epileptology, Fondazione Istituto Neurologico Carlo Besta). Current source density (CSD) analysis was performed on laminar field potential profiles with a 200 / 400 μm separation grid in order to distinguish local activities from volume-conducted far fields (Biella & de Curtis, 2000).

Evoked responses after stimulation of the lateral olfactory tract (LOT) (see Biella & de Curtis, 2000) were monitored during the experiment (Fujiwara-Tsukamoto *et al.*, 2007). Stimuli were delivered through an isolation unit driven by a pulse generator (Telefactor S88; Grass, Warwick, RI, USA). Stimulating and recording electrodes were positioned under direct visual control with a stereoscopic microscope. To reconstruct the position of the 16-channel silicon probe, electrolytic lesions were performed at the end of the experiment by passing current between the two deepest recording sites of the probes (15 V for 1 min). Brains were then immersed in paraformaldehyde 4% for 1 week, cut into 75-μm-thick sections and counterstained with thionine.

The 4AP (20–50 μM; Fluka, Milan, Italy), glutamatergic AMPA receptor antagonists 6-cyano-7-nitroquinoxaline-2,3-dione (CNQX) (50 μM; Sigma-Aldrich, Milan, Italy) and 6,7-dinitroquinoxaline-2,3-dione (DNQX) (50 μM; Sigma-Aldrich), NMDA receptor antagonists 2-amino-5-phosphonopentanoic acid (AP5) (Sigma-Aldrich) and 3(−2 carboxipiperazin-4-yl)-propyl-1-phosphonic acid (CPP) (Sigma-Aldrich), and the $GABA_A$ receptor antagonist

bicuculline methiodide (50 μM; Sigma-Aldrich) were dissolved in the perfusate and applied via the resident arterial system.

Results

Effects of 4-aminopyridine on synaptic potentials and propagation

We characterized the effects of 4AP on network excitability by analysing the propagation of the activity evoked by stimulation of the LOT in the olfactory-limbic region. Under control conditions LOT stimulation induced a monosynaptic / disynaptic field response in the PC followed by polysynaptic propagation to the l-EC and hippocampus (Fig. 1). We have previously reported that, only when repetitive stimulation at 2–8 Hz is performed, activity further propagates to the CA1 region of the hippocampus and from here back to the medial part of the EC (Biella & de Curtis, 2000; Biella *et al.*, 2003). Simultaneous extracellular recordings obtained from the PC, l-EC and m-EC, and in the CA1 region of the hippocampus demonstrated that 4AP (50 μM) enhanced the propagation of the responses evoked by a single LOT stimulus and promoted re-entrant activation of the m-EC (Fig. 1) via the trisynaptic hippocampal loop (Biella & de Curtis, 2000; Biella *et al.*, 2003). In eight out of 12 experiments the PC response during 4AP showed an additional delayed component that peaked at 65.02 ± 13.70 ms (asterisks in Figs 1 and 2A). CSD analysis performed on PC laminar profiles with 16-channel silicon probes confirmed that this delayed component induced by 4AP was localized in the superficial layers of the PC (asterisk in Fig. 2C, $n = 3$).

To further evaluate the network changes induced by 4AP in olfactory-limbic circuits we utilized paired-pulse LOT stimulation. We compared the amplitudes of monosynaptic and disynaptic responses in the PC during conditioning (first) and conditioned (second) paired stimuli. Under control conditions, paired-pulse stimulation of the LOT with interstimulus intervals (ISIs) between 10 and 50 ms induced a decrease in amplitude of the disynaptic component in the second response (control panels in Fig. 2A and B) [the disynaptic potential recovered for ISIs longer than 50 ms (thin arrows in the control panel in Fig. 2A)]. Perfusion with 4AP prolonged the inhibition of the disynaptic component in the second response (right panel in Fig. 2A; $n = 7$) that remained significantly reduced to 43.86 ± 42.81% at an ISI of 70–80 ms (black column in Fig. 2B; paired *t*-test, $P < 0.05$).

To isolate the potential evoked by the second stimulus in a pairing test (trace b–a in Fig. 2C), the trace recorded after paired-pulse stimulation (trace b in Fig. 2C) with a 20 ms ISI was subtracted from the single-pulse response trace (trace a in Fig. 2C). CSD analysis performed on b–a field profiles demonstrated that the current sink associated with the isolated second field potential localized in the most superficial 100 μm of the PC (right panel in Fig. 2C). The latency and depth location of the CSD sink confirmed the monosynaptic nature of this potential localized in layer I (Ketchum & Haberly, 1993; Biella & de Curtis, 1995). Perfusion of 4AP also induced the complete disappearance of the conditioned response evoked by paired LOT stimulation in the l-EC and hippocampus (Fig. 2D; $n = 7$). The same effect was obtained with ISIs as long as 200 ms (not shown) and with lower doses of 4AP (10–25 μM; $n = 5$). These results suggest that local inhibitory networks are more efficient during 4AP application and prevent propagation of repetitive evoked excitation along a polysynaptic pathway. However, in spite of the enhanced inhibition demonstrated above,

spontaneous interictal and ictal epileptiform discharges (Fig. 3) were consistently observed during 4AP application, suggesting that excitation is also potentiated by 4AP. Seizure-like discharges appeared with a delay of 4.99 ± 1.6 min from the beginning of the perfusion with 4AP and had a duration of 2.41 ± 1.14 min ($n = 7$). Seizure-like activity did not engage the PC (Fig. 3) and propagated bilaterally to the hippocampus / EC region.

Pharmacology of 4-aminopyridine-induced activity

The LOT-evoked field responses were abolished by co-perfusion of 4AP with the glutamate receptor antagonists DNQX (20–50 μM, $n = 12$) and AP5 (100 μM; $n = 14$; Fig. 4A). Similar effects were observed when DNQX was replaced with CNQX (10 μM; $n = 5$) and AP5 with 3(−2 carboxipiperazin-4-yl)-propyl-1-phosphonic acid (20–50 μM; $n = 3$). LOT-evoked responses were also abolished when 4AP perfusion was preceded by prolonged (30 min) application of DNQX (or CNQX) and AP5 (or CPP) ($n = 10$; Fig. 4B). Epileptiform activity was suppressed by perfusion of glutamate receptor antagonists (see Fig. 5A; $n = 3$) and was prevented when DNQX (or CNQX) and AP5 [or 3(−2 carboxipiperazin-4-yl)-propyl-1-phosphonic acid] perfusion preceded 4AP application (not shown; $n = 10$).

After 7.47 ± 2.34 min of perfusion with 4AP and glutamate receptor blockers, large amplitude spontaneous potentials appeared in both the hippocampus and EC ($n = 17$), as shown in Fig. 5A (4AP + DNQX + AP5 panel). To test their sensitivity to $GABA_A$ receptor antagonists, bicuculline methiodide (50 μM) was applied to the 4AP+glutamate receptor blockers solution. This pharmacological procedure either abolished ($n = 4$) or dramatically reduced ($n = 6$) the spontaneous potentials (Fig. 5A, 4AP + DNQX + AP5 + BIC panel). The effect of bicuculline partially recovered upon washout (not shown). Arterial perfusion with the NMDA receptor antagonist AP5 (100 μM) also reduced or abolished the delayed potential observed in the PC during 4AP ($n = 7$; not shown).

Further analysis based on the propagation properties of spontaneous bicuculline-sensitive events allowed the identification of two types of potentials: type 1 potentials were observed in the hippocampus only, whereas type 2 events propagated within the entorhinal / hippocampal circuit (Fig. 5B). In three experiments, type 2 activity also propagated to the l-EC (Fig. 5A) and in six experiments to the PC. Both propagating and non-propagating potentials were observed in the same experiment ($n = 13$), with the exception of three experiments in which only type 2 potentials were recorded and one experiment in which only type 1 was identified. Type 1 potentials located in the dentate gyrus (DG) and CA3 showed variable duration (500–1500 ms) and recurred every 15–30 s. When recordings were performed in both hemispheres, type 1 potentials could be generated independently in the two hippocampi and did not propagate to the contralateral side ($n = 9$). Type 2 potentials occurred in either the hippocampus or m-EC, usually lasted less than 500 ms, showed a periodicity of *c.* 20 s and could propagate between hemispheres (Fig. 5B and C).

By comparing the time onset of the field potentials recorded in the EC and hippocampus, we found that 74% of the potentials originated in the m-EC (Fig. 6A). We estimated the onset delays of the potential recorded in both the m-EC and different subfields of the hippocampus (as shown in Fig. 6B). To locate the potentials recorded in the hippocampus, we analysed only experiments in which CSD of laminar profiles was performed and compared the onset

of the m-EC potential with the onset of the hippocampal sinks. We found a short delay between the m-EC potential and the potential recorded in the DG / CA1 region, and an increased delay when the multielectrode was positioned across the hilus of the DG and CA3. More variable delays were found when the onset of potentials originating in the m-EC and propagating to the contralateral side was considered (Fig. 6C).

Current source density and intracellular analysis of the 4-aminopyridine-induced glutamatergic-independent activity

The CSD analysis was performed on laminar profiles obtained with 16-channel silicon probes (100 μm separation) to localize the active synaptic sites responsible for the generation of the glutamatergic-independent, bicuculline-sensitive potentials. CSD confirmed that both type 1 and type 2 potentials were locally generated in different subfields of the hippocampus, whereas only type 2 potentials originated in the m-EC. CSD analysis demonstrated that type 1 and type 2 potentials recorded in the same experiment were sustained by distinct circuits. In the representative experiment illustrated in Fig. 7A, a type 1 potential (Fig. 7A, b) and a type 2 potential (Fig. 7A, c) were associated with current sinks located in the DG and CA3 region, respectively. CSD analysis of the type 2 field potential recorded in the m-EC confirmed that it was locally generated in the m-EC and propagated to the hippocampus (Fig. 7B).

To understand the mechanisms of generation of the GABAergic potentials, intracellular recordings were performed in the most accessible structure of the limbic region, the m-EC, where both locally generated and propagated events were recorded. Intracellular and juxtacellular recordings (performed from 17 and 9 principal EC neurons, respectively) demonstrated that type 2 $GABA_A$-receptor-mediated interictal potentials originating in the EC (Fig. 8A, a), as well as those propagating to the EC (Fig. 8A, b), correlated with a hyperpolarizing inhibitory potential that was interrupted by a series of action potentials. These inhibitory postsynaptic potentials (IPSPs) had a peak amplitude at 38.61 ± 22.48 ms, showed a membrane potential reversal at −68.12 ± 8.01 mV ($n = 5$) and lasted 766.72 ± 502.90 ms ($n = 14$). Series of action potentials (from 1 to 20 spikes at a frequency of 50–100 Hz) initiated 39.77 ± 23.14 ms after the onset of the IPSPs and did not alter the time course. Action potentials did not show the features of postinhibitory spikes and had an abrupt onset break that did not rise on excitatory synaptic potentials. In four out of eight neurons these spikes showed lower amplitudes when compared with the spikes induced by depolarizing current pulses. These features suggest an ectopic origin for these action potentials.

Discussion

We confirm here that arterial perfusion of the potassium channel blocker 4AP in the *in-vitro* isolated guinea pig brain preparation facilitates both excitatory and inhibitory synaptic activities in the olfactory-limbic cortices. In this acute model of ictogenesis, enhanced synaptic neurotransmission is suggested by the enhancement of activity propagation along the PC / EC / hippocampal pathway during single-shock stimuli and by the induction of epileptiform potentials. Increased synaptic inhibition is supported by the demonstration of

(i) depression of disynaptic potentials evoked by paired LOT stimulation, (ii) decreased polysynaptic responses to paired stimuli and (iii) induction of spontaneous potentials resistant to ionotropic glutamatergic antagonists and sensitive to $GABA_A$ receptor antagonism.

The 4AP enhanced the propagation of excitation along the polysynaptic pathway activated by LOT stimulation that sequentially involves the PC, l-EC and hippocampal trisynaptic pathway (Biella & de Curtis, 2000). Therefore, 4AP facilitated propagation of activity, as during repetitive olfactory stimulation at theta frequency (Biella & de Curtis, 2000). However, 4AP also induced an enhancement of inhibitory potentials. To study synaptic network inhibition, we performed paired-pulse analysis of LOT responses. When the same LOT stimulus was repeated with a 20–30 ms interval, disynaptic activity was depressed in the second response. This is due to the coincident activation of mainly recurrent inhibition evoked by the first (conditioning) stimulus during the monosynaptic activation induced by the second stimulus of the pair; neuronal firing is prevented in this condition and disynaptic potentials are blocked (Dunwiddie *et al.*, 1986; Biella *et al.*, 1996). The duration of this phenomenon depends on the duration of the recurrent inhibitory potential that prevents somatic reactivation. Under control condition, the depression of the disynaptic second component recovered at an ISI of 70 ms, whereas in the presence of 4AP depression was still present with an ISI of 70–200 ms. These findings suggest that recurrent inhibition is enhanced by 4AP. As the duration of paired-pulse depression of disynaptic potential coincides with the duration of the delayed slow potential illustrated in Figs 1 and 2C, we are inclined to propose that the latter represents, at least in part, the extracellular correlate of enhanced inhibition in the PC (see also Rodriguez & Haberly, 1989; Ketchum & Haberly, 1993; Kanter *et al.*, 1996). Previous studies demonstrated that a delayed potential with similar features could be induced by bicuculline, and was mediated by intracortical associative interactions (de Curtis *et al.*, 1996) via NMDA receptors (Forti *et al.*, 1997). These findings were confirmed in the present model by arterial perfusion with the NMDA receptor antagonist AP5. Therefore, we conclude that the delayed potential in the PC represents an enhancement of both inhibitory and excitatory synaptic responses.

The non-NMDA and NMDA glutamate receptor antagonists DNQX and AP5 (or the analogues CNQX and CPP) administered before or together with 4AP determined the suppression of all of the components of LOT-evoked responses and also of epileptiform discharges. Co-perfusion of 4AP and glutamate receptor blockers revealed spontaneous potentials that exhibited sensitivity to the $GABA_A$ receptor antagonist bicuculline, demonstrating that they were GABA-receptor-mediated. Two types of synchronous inhibitory GABAergic potentials were classified according to their propensity to propagate. Type 1 potentials were isolated into subfields of the hippocampus proper, whereas the type 2 potentials propagated along the entorhinal / hippocampal circuits bilaterally. Type 2 potentials originated in both the m-EC and hippocampus, and showed a clear prevalence (74%) in the m-EC. This observation is in line with evidence obtained in combined EC / hippocampal slices (Avoli *et al.*, 1996).

In the present study, experiments were performed at 32°C because mild hypothermia was employed as a substitute for anesthesia in the isolated guinea pig brain (see de Curtis *et al.*,

1991, 1998). Neurotransmission and other excitability processes are slowed at this temperature (Ginsberg *et al.*, 1993). However, a considerable number of studies performed in the *in-vitro* isolated guinea pig brain demonstrated that intracellularly recorded inhibitory potentials and extracellular current sinks and sources show general features (duration, time course, amplitude, etc.) that are similar to those reported *in vivo* (Biella & de Curtis, 1995; Biella *et al.*, 2002; Gnatkovsky *et al.*, 2008). Moreover, mild hypothermia does not prevent the generation of complex network patterns, such as periodic spontaneous events similar to the up-down states observed *in vivo* during anesthesia (Dickson *et al.*, 2003; Gnatkovsky *et al.*, 2007), that require fast and synchronous synaptic interactions between principal cells and interneurons.

Previous findings have demonstrated that synchronous GABA potentials can be induced by 4AP (Avoli *et al.*, 1996; Lopantsev & Avoli, 1998), Mg^{2+} withdrawal (Köhling *et al.*, 2000), tetanic stimulation (Kaila *et al.*, 1997; Pignataro *et al.*, 2007) or GABA uptake inhibition and also in neurons from human epileptic subiculum (Cohen *et al.*, 2002). In guinea pig slices, Michelson & Wong (1994) demonstrated the occurrence of a triphasic IPSP in the pyramidal cell layers of CA3 and CA1, and in the granule cell layer of DG in the presence of 4AP and glutamate receptor blockers; the hyperpolarization of the principal cells was due to interneurons that were able to recruit other interneurons via depolarizing $GABA_A$-receptor-mediated conductance. Similar sequences of hyperpolarization / depolarization/ hyperpolarization during 4AP were also shown in rat CA1 cells (Perreault & Avoli, 1989; Lamsa & Kaila, 1997) or EC neurons (Lopantsev & Avoli, 1998). Depolarizing GABA, however, does not seem to have a role in the interictal GABAergic potential observed in our experiments, as intracellular recordings from principal EC neurons revealed hyperpolarizing inhibitory potential with the typical reversal of $GABA_A$-receptor-mediated IPSPs.

Interestingly, the IPSPs were interrupted by a series of action potentials that presumably did not emerge from excitatory synaptic mechanisms. Several features of this type of firing suggest that it was ectopically generated. First, they lacked a prepotential component and thus displayed an abrupt onset break. Second, they often had lower amplitudes than the action potentials induced by depolarizing current pulses in the same cell. Third, either at resting membrane potential or during active depolarization of the membrane potential with injection of current, they occurred in coincidence with the hyperpolarizing component of the IPSP that reflected the GABA-receptor-mediated field event at the intracellular level. These features, which are similar to those reported in CA1 pyramidal cells in a slice preparation during 4AP treatment (Perreault & Avoli, 1989; Avoli *et al.*, 1998), suggest an ectopic origin for these action potentials (Stasheff *et al.*, 1993). It has been proposed that action potentials during the synchronous GABA-receptor-dependent potential are generated at ectopic sites, such as axonal terminals, because of the transient increases in $[K^+]_O$ (Avoli *et al.*, 1998). An intriguing issue is to understand how type 2 GABAergic potentials propagate within the entorhinal / hippocampal circuit during suppression of excitatory synaptic transmission. Propagation may occur either via long-projection GABAergic pathways or via non-synaptic mechanisms. The intracellular recordings obtained in the isolated guinea pig brain have shown that the GABAergic potential is associated with IPSPs that are known to be accompanied by transient increases in $[K^+]_O$ (Avoli *et al.*, 1996; Morris *et al.*, 1996; Lamsa & Kaila, 1997), due to activation of $GABA_A$ receptors with low affinity. An increase of [K

$^{+}]_O$ is known to promote the depolarization of neurons, supporting the generation of ectopic, non-synaptic firing in nearby principal cells and interneurons. Moreover, activity-dependent pH shifts may also play a role. The principal pH buffer of the extracellular fluid is CO_2 / HCO_3^-. The efflux of HCO_3^- through the $GABA_A$ receptors during IPSPs results in an intracellular acidification and extracellular alkalinization (Church & McLennan, 1989; Chen & Chesler, 1992; Lamsa & Kaila, 1997). These pH changes could, in principle, enhance cellular excitability via modulation of both voltage-dependent and ligand-gated channel functions (Iijima *et al.*, 1986; Aram & Lodge, 1987; Balestrino & Somjen, 1988; Traynelis & Cull-Candy, 1990; Pasternack *et al.*, 1996; Tombaugh & Somjen, 1996; Tombaugh, 1998; Chesler, 2003). These effects could hypothetically contribute via non-synaptic mechanisms to the generation of neuronal firing in groups of principal cells and interneurons. This sequence of events is suggested by the intracellular recordings performed in principal EC neurons. The GABA-mediated field potential correlated with a large IPSP interrupted by a series of possibly ectopic action potentials. In the absence of glutamatergic neurotransmission only GABAergic synapses activate, therefore reinforcing a recurrent loop that could be large and synchronous enough to generate a field response. Interestingly, the GABAergic potential observed in our experiments featured a negative peak potential that correlated in time with the ectopic firing observed at the intracellular level in principal neurons. Non-synaptically-mediated propagation of firing across neurons may occur, for instance via principal-to-interneuron gap junctions, and could contribute to further local recruitment of inhibitory neurons during the GABAergic potential.

Similar mechanisms could also sustain the propagation of GABAergic potentials between different regions of the limbic system. Massive firing of inhibitory cells that project at distance onto GABAeric neurons may contribute to the propagation of GABAergic potentials and could reproduce similar sequences of events in limbic regions that are remote from the site where the GABAergic potential initially originated. If this hypothesis is correct, it could be anticipated that long-projection interneurons in the EC are possibly supporting propagation of type 2 potentials, whereas the lack of long-range inhibitory interneurons in the hippocampus (where type 1 potentials are most often recorded) may explain their inability to propagate. However, no indications regarding this are available in the literature. As spared inhibition has been reported to characterize the early phases of temporal lobe epileptogenesis (Du *et al.*, 1995; Eid *et al.*, 1999), our findings suggest a potential role of GABA-mediated synchronization in epileptogenesis.

Acknowledgments

This study was supported by the Italian Health Ministry (Ricerca Corrente e Ricerca Finalizzata RF 64), the Pierfranco and Maria Luisa Mariani Foundation (grant no. R06-50), the Canadian Institutes of Health Research (CIHR; grant 8109), and the Savoy Foundation.

Abbreviations

4AP	4-aminopyridine
AP5	2-amino-5-phosphonopentanoic acid
CNQX	6-cyano-7-nitroquinoxaline-2,3-dione

CPP	3(-2 carboxipiperazin-4-yl)-propyl-1-phosphonic acid
CSD	current source density
DG	dentate gyrus
DNQX	6,7-dinitroquinoxaline-2,3-dione
EC	entorhinal cortex
IPSP	inhibitory postsynaptic potential
ISI	interstimulus interval
l-EC	lateral entorhinal cortex
LOT	lateral olfactory tract
m-EC	medial entorhinal cortex
NMDA	*N*-methyl-d-aspartate
PC	piriform cortex

References

Aram JA, Lodge D. Epileptiform activity induced by alkalosis in rat neocortical slices: block by antagonists of N-methyl-D-aspartate. Neurosci Lett. 1987; 83:345–350. [PubMed: 2894627]

Aram JA, Michelson HB, Wong RKS. Synchronized GABAergic IPSPs recorded in the neocortex after blockade of synaptic transmission mediated by excitatory amino acids. J Neurophysiol. 1991; 65:1034–1041. [PubMed: 1678421]

Avoli M, Mattia D, Siniscalchi A, Perreault P, Tomaiuolo F. Pharmacology and electrophysiology of a synchronous GABA-mediated potential in the human neocortex. Neuroscience. 1994; 62:655–666. [PubMed: 7870297]

Avoli M, Barbarosie M, Lücke A, Nagao T, Lopantsev V, Köhling R. Synchronous GABA-mediated potentials and epileptiform discharges in the rat limbic system in vitro. J Neurosci. 1996; 16:3912–3924. [PubMed: 8656285]

Avoli M, Methot M, Kawasaki H. GABA-dependent generation of ectopic action potentials in the rat hippocampus. Eur J Neurosci. 1998; 10:2714–2722. [PubMed: 9767401]

Avoli M, D'Antuono M, Louvel J, Kohling R, Biagini G, Pumain R, D'Arcangelo G, Tancredi V. Network pharmachological mechanisms leading to epileptiform synchronization in the limbic system in vitro. Progr Neurobiol. 2002; 68:167–207.

Balestrino M, Somjen GG. Concentration of carbon dioxide, interstitial pH and synaptic transmission in hippocampal formation of the rat. J Physiol. 1988; 396:247–266. [PubMed: 2842490]

Bender RA, Kirschstein T, Kretz O, Brewster AL, Richichi C, Ruschenschmidt C, Shigemoto R, Beck H, Frotscher M, Baram TZ. Localization of HCN1 channels to presynaptic compartments: novel plasticity that may contribute to hippocampal maturation. J Neurosci. 2007; 27:4697–4706. [PubMed: 17460082]

Biella G, de Curtis M. Associative synaptic potentials in the piriform cortex of the isolated guinea-pig brain in vitro. Eur J Neurosci. 1995; 7:54–64. [PubMed: 7711937]

Biella G, de Curtis M. Olfactory inputs activate the medial entorhinal cortex via the hippocampus. J Neurophysiol. 2000; 83:1924–1931. [PubMed: 10758103]

Biella G, Panzica F, de Curtis M. Interactions between associative synaptic potentials in the piriform cortex of the in vitro isolated guinea pig brain. Eur J Neurosci. 1996; 8:1350–1357. [PubMed: 8758942]

Biella G, Uva L, de Curtis M. Network activity evoked by neocortical stimulation in area 36 of the guinea pig perirhinal cortex. J Neurophysiol. 2001; 86:164–172. [PubMed: 11431498]

Biella G, Uva L, de Curtis M. Propagation of neuronal activity along the neocortical-perirhinal-entorhinal pathway in the guinea pig. J Neurosci. 2002; 22:9972–9979. [PubMed: 12427854]

Biella G, Gnatkovsky V, Takashima I, Kajiwara R, Iijima T, De Curtis M. Olfactory input to the parahippocampal region of the isolated guinea pig brain reveals weak entorhinal-to-perirhinal interactions. Eur J Neurosci. 2003; 18:95–101. [PubMed: 12859341]

Chen JC, Chesler M. pH transients evoked by excitatory synaptic transmission are increased by inhibition of extracellular carbonic anhydrase. Proc Natl Acad Sci USA. 1992; 89:7786–7790. [PubMed: 1380165]

Chesler M. Regulation and modulation of pH in the brain. Physiol Rev. 2003; 83:1183–1221. [PubMed: 14506304]

Church J, McLennan H. Electrophysiological properties of rat CA1 pyramidal neurones in vitro modified by changes in extracellular bicarbonate. J Physiol. 1989; 415:85–108. [PubMed: 2561793]

Cohen I, Navarro V, Clemenceau S, Baulac M, Miles R. On the origin of interictal activity in human temporal lobe epilepsy in vitro. Science. 2002; 298:1418–1421. [PubMed: 12434059]

de Curtis M, Pare D, Llinas RR. The electrophysiology of the olfactory-hippocampal circuit in the isolated and perfused adult mammalian brain in vitro. Hippocampus. 1991; 1:341–354. [PubMed: 1669314]

de Curtis M, Biella G, Forti M. Epileptiform activity in the piriform cortex of the in vitro isolated guinea pig brain preparation. Epilepsy Res. 1996; 26:75–80. [PubMed: 8985689]

de Curtis M, Biella G, Buccellati C, Folco G. Simultaneous investigation of the neuronal and vascular compartments in the guinea pig brain isolated in vitro. Brain Res Protoc. 1998; 3:221–228.

D'Antuono M, Louvel J, Kohling R, Mattia D, Bernasconi A, Olivier A, Turak B, Devaux A, Pumain R, Avoli M. GABAA receptor-dependent synchronization leads to ictogenesis in the human dysplastic cortex. Brain. 2004; 127:1626–1640. [PubMed: 15175227]

Dickson CT, Biella G, de Curtis M. Slow periodic events and their transition to fast gamma oscillations in the entorhinal cortex of the isolated guinea-pig brain. J Neurophysiol. 2003; 90:39–46. [PubMed: 12843303]

Du F, Eid T, Lothman EW, Köhler C, Schwarcz R. Preferential neuronal loss in layer III of the medial entorhinal cortex in rat models of temporal lobe epilepsy. J Neurosci. 1995; 15:6301–6313. [PubMed: 7472396]

Dunwiddie TV, Worth TS, Olsen RW. Facilitation of recurrent inhibition in rat hippocampus by barbiturate and related nonbarbiturate depressant drugs. J Pharmacol Exp Ther. 1986; 238:564–575. [PubMed: 3735132]

Eid T, Schwarcz R, Ottersen OP. Ultrastructure and immunocytochemical distribution of GABA in layer III of the rat medial entorhinal cortex following aminooxyacetic acid-induced seizures. Exp Brain Res. 1999; 125:463–475. [PubMed: 10323293]

Forti M, Biella G, Caccia S, de Curtis M. Persistent excitability changes in the piriform cortex of the isolated guinea pig brain preparation after transient exposure to bicuculline. Eur J Neurosci. 1997; 9:435–451. [PubMed: 9104586]

Fujiwara-Tsukamoto Y, Isomura Y, Imanishi M, Fukai T, Takada M. Distinct types of ionic modulation of GABA actions in pyramidal cells and interneurons during electrical induction of hippocampal seizure-like network activity. Eur J Neurosci. 2007; 25:2713–2725. [PubMed: 17459104]

Ginsberg MD, Globus MY, Dietrich WD, Busto R. Temperature modulation of ischemic brain injury – a synthesis of recent advances. Prog Brain Res. 1993; 96:13–22. [PubMed: 8101386]

Gnatkovsky V, Wendling F, de Curtis M. Spontaneous periodic oscillatory events are generated by superficial neurons in medial entorhinal cortex of the isolated guinea pig brain. Eur J Neurosci. 2007; 26:302–311. [PubMed: 17650108]

Gnatkovsky V, Uva L, de Curtis M. Intracellular recordings of the medial entorhinal cortex neurons during fast oscillatory activity at ictal epileptiform discharge onset in isolated guinea pig brain preparation. Ann Neurol. 2008; 64:674–686. [PubMed: 19107991]

Huberfeld G, Wittner L, Clemenceau S, Baulac M, Kaila K, Miles R, Rivera C. Perturbed chloride homeostasis and GABAergic signaling in human temporal lobe epilepsy. J Neurosci. 2007; 27:9866–9873. [PubMed: 17855601]

Iijima T, Ciani S, Hagiwara S. Effects of the external pH on Ca channels: experimental studies and theoretical considerations using a two-site, two-ion model. Proc Natl Acad Sci USA. 1986; 83:654–658. [PubMed: 2418439]

Kaila K, Lamsa K, Smirnov S, Taira T, Voipio J. Long-lasting GABA-mediated depolarization evoked by high-frequency stimulation in pyramidal neurons of rat hippocampal slice is attributable to a network-driven, bicarbonate-dependent K^+ transient. J Neurosci. 1997; 17:7662–7672. [PubMed: 9315888]

Kanter ED, Kapur A, Haberly LB. A dendritic GABAa-mediated IPSP regulates facilitation of NMDA-mediated responses to burst stimulation of afferent fibers in piriform cortex. J Neurophysiol. 1996; 16:307–312.

Ketchum KL, Haberly LB. Membrane currents evoked by afferent fiber stimulation in rat piriform cortex. I Current source-density analysis. J Neurophysiol. 1993; 69:248–260. [PubMed: 8381858]

Klaassen A, Glykys J, Maguire J, Labarca C, Mody I, Boulter J. Seizures and enhanced cortical GABAergic inhibition in two mouse models of human autosomal dominant nocturnal frontal lobe epilepsy. Proc Natl Acad Sci USA. 2006; 103:19152–19157. [PubMed: 17146052]

Kohling R, Lucke A, Straub H, Speckmann EJ, Tuxhorn I, Wolf P, Pannek H, Oppel F. Spontaneous sharp waves in human neocortical slices excised from epileptic patients. Brain. 1998; 121:1073–1087. [PubMed: 9648543]

Köhling R, Vreugdenhl M, Bracci E, Jefferys JGR. Ictal epileptiform activity is facilitated by hippocampal $GABA_A$ receptor-mediated oscillations. J Neurosci. 2000; 20:6820–6829. [PubMed: 10995826]

Lamsa K, Kaila K. Ionic mechanisms of spontaneous GABAergic events in rat hippocampal slices exposed to 4-aminopyridine. J Neurophysiol. 1997; 78:2582–2591. [PubMed: 9356408]

Llinas R, Yarom Y, Sugimori M. Isolated mammalian brain in vitro: new technique for analysis of electrical activity of neuronal circuit function. Fed Proc. 1981; 40:2240–2245. [PubMed: 7238908]

Lopantsev V, Avoli M. Participation of GABAA-mediated inhibition in ictallike discharges in the rat entorhinal cortex. J Neurophysiol. 1998; 79:352–360. [PubMed: 9425204]

Louvel J, Papatheodoropoulos C, Siniscalchi A, Kurcewicz I, Pumain R, Devaux B, Turak B, Esposito V, Villemeure JG, Avoli M. GABA-mediated synchronization in the human neocortex: elevations in extracellular potassium and presynaptic mechanisms. Neuroscience. 2001; 105:803–813. [PubMed: 11530219]

Michelson HB, Wong RKS. Excitatory synaptic responses mediated by $GABA_A$ receptors in the hippocampus. Science. 1991; 253:1420–1423. [PubMed: 1654594]

Michelson HB, Wong RK. Synchronization of inhibitory neurones in the guinea-pig hippocampus in vitro. J Physiol (Lond). 1994; 477:35–45. [PubMed: 8071887]

Morris ME, Obrocea GV, Avoli M. Extracellular K^+ accumulations and synchronous GABA-mediated potentials evoked by 4-aminopyridine in the adult rat hippocampus. Exp Brain Res. 1996; 109:71–82. [PubMed: 8740210]

Muhlethaler M, de Curtis M, Walton K, Llinas R. The isolated and perfused brain of the guinea-pig in vitro. Eur J Neurosci. 1993; 5:915–926. [PubMed: 8281302]

Pasternack M, Smirnov S, Kaila K. Proton modulation of functionally distinct GABAA receptors in acutely isolated pyramidal neurons of rat hippocampus. Neuropharmacology. 1996; 35:1279–1288. [PubMed: 9014143]

Pearcy WC, Virtue RW. Multichannel EEG in hypothermia and circulatory occlusion. Anesthesiology. 1960; 21:35–39. [PubMed: 14431224]

Perrault P, Avoli M. 4-Aminopyridine-induced activity in hilar neurons in the guinea pig hippocampal slice. J Neurosci. 1992; 12:104–115. [PubMed: 1309571]

Perreault P, Avoli M. Effects of low concentrations of 4-aminopyridine on CA1 pyramidal cells of the hippocampus. J Neurophysiol. 1989; 61:953–970. [PubMed: 2566657]

Perreault P, Avoli M. Physiology and pharmacology of epileptiform activity induced by 4-aminopyridine in rat hippocampal slices. J Neurophysiol. 1991; 65:771–785. [PubMed: 1675671]

Pignataro G, Studer FE, Wilz A, Simon RP, Boison D. Neuroprotection in ischemic mouse brain induced by stem cell-derived brain implants. J Cereb Blood Flow Metab. 2007; 27:919–927. [PubMed: 17119544]

Rodriguez R, Haberly LB. Analysis of synaptic events in the opossum piriform cortex with improved CSD technique. J Neurophysiol. 1989; 61:702–718. [PubMed: 2723716]

Stasheff SF, Hines M, Wilson WA. Axon terminal hyperexcitability associated with epileptogenesis in vitro. I Origin of ectopic spikes. J Neurophysiol. 1993; 70:961–975. [PubMed: 8229182]

Sudbury JR, Avoli M. Epileptiform synchronization in the rat insular and perirhinal cortices in vitro. Eur J Neurosci. 2007; 26:3571–3582. [PubMed: 18052975]

Tombaugh GC. Intracellular pH buffering shapes activity-dependent $Ca2^{+}$ dynamics in dendrites of CA1 interneurons. J Neurophysiol. 1998; 80:1702–1712. [PubMed: 9772233]

Tombaugh GC, Somjen GG. Effects of extracellular pH on voltage-gated Na^{+}, K^{+} and $Ca2^{+}$ currents in isolated rat CA1 neurons. J Physiol. 1996; 493:719–732. [PubMed: 8799894]

Traynelis SF, Cull-Candy SG. Proton inhibition of N-methyl-D-aspartate receptors in cerebellar neurons. Nature. 1990; 345:347–350. [PubMed: 1692970]

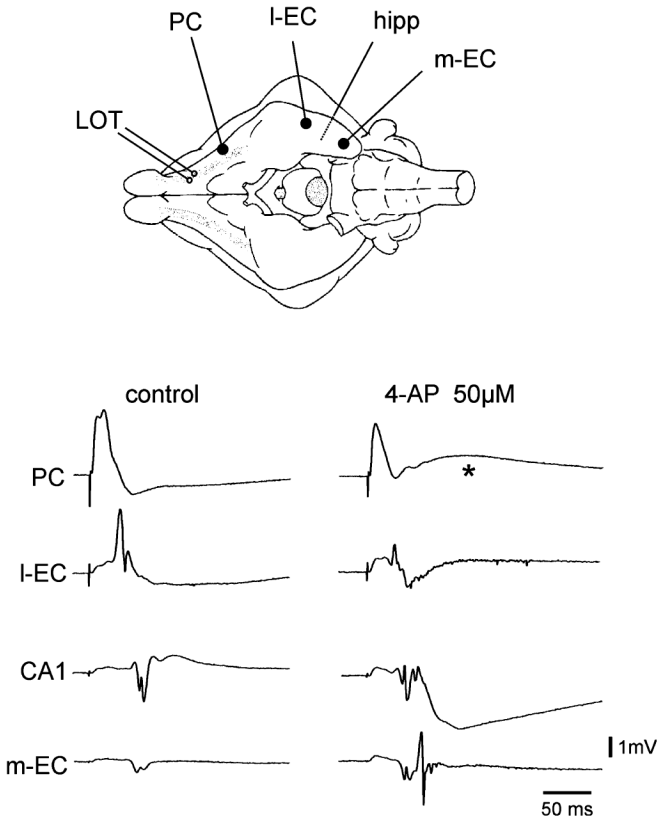

Fig. 1.

Stimulation of the LOT induces the sequential activation of the PC, l-EC and subfield CA1 of the hippocampus under control conditions. Note that perfusion with 4AP induces further re-entrant propagation of LOT-evoked activity from the hippocampus to the m-EC. The asterisk indicates the delayed slow potential induced by 4AP in the PC. The scheme of the position of the electrode is illustrated in the upper panel.

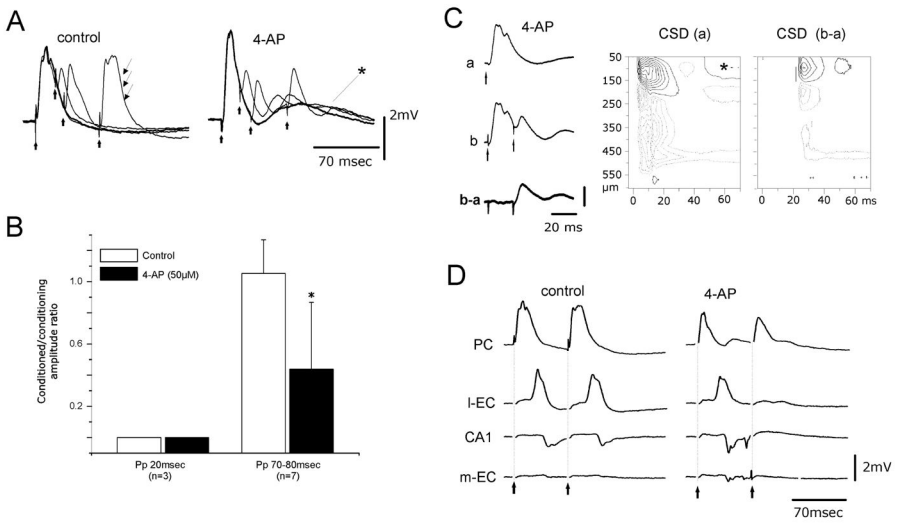

Fig. 2.

(A) Paired-pulse (Pp) stimulation with different ISIs induces suppression of disynaptic potentials in the conditioned PC response. The disynaptic component (arrows) recovers at an ISI of 70 ms under control conditions. During perfusion with 4AP the paired-pulse depression of disynaptic potential did not recover at an ISI of 70 ms. The asterisk marks the delayed slow potential induced by 4AP in the PC. (B) Ratio between the amplitudes of the conditioned (second) and the conditioning (first) disynaptic components at ISIs of 20 and 70–80 ms in control solution (gray columns) and during 4AP application (black columns). (C) PC response to single stimulation (a) and to paired-pulse stimulation at 20 ms ISI (b), and digitally subtracted trace (b–a). The CSD contour plot of the b–a laminar profile shows that only the monosynaptic components located in the most superficial cortex remain after the conditioned stimulus. Isocurrent lines at 0.14 mV / mm^2. (D) Field potentials simultaneously recorded in the PC, l-EC, CA1 and m-EC after double-pulse stimulation of the LOT in control condition and during 4AP perfusion. 4AP blocks the propagation of activity evoked by the second stimulus of the pair.

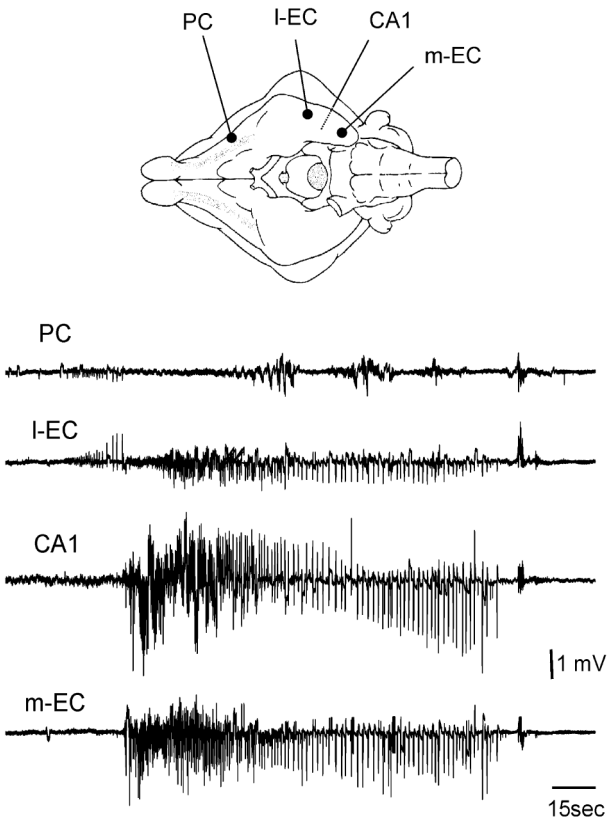

Fig. 3.

Epileptiform ictal discharges recorded during 4AP perfusion. Simultaneous extracellular recordings were obtained from the PC, l-EC, CA1 region of the hippocampus and m-EC. The ictal discharge originates from the l-EC and propagates to the hippocampus and m-EC. The scheme of the position of the electrodes is illustrated in the upper panel.

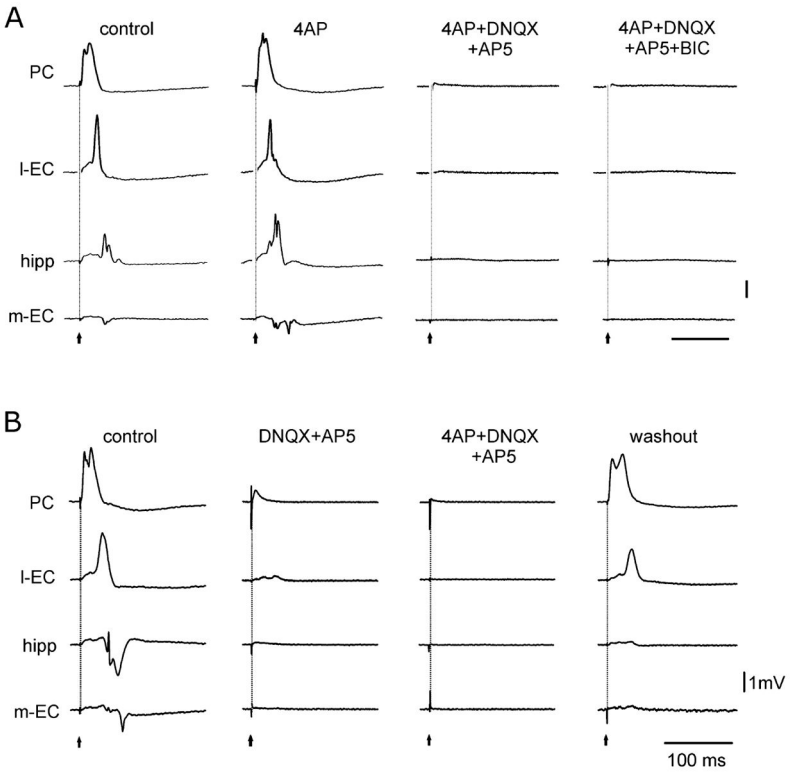

Fig. 4.

(A) Modification of the LOT-evoked responses in the PC, l-EC, hippocampus (CA1) and m-EC during application of 4AP alone or co-perfusion with glutamatergic and $GABA_A$ receptor antagonists. Note that glutamatergic receptor antagonism [DNQX (50 μM) and AP5 (100 μM)] abolishes the evoked response. Additional perfusion of bicuculline (BIC) (50 μM) does not change the response. (B) Arterial perfusion of the glutamatergic receptor blockers DNQX (50 μM) and AP5 (100 μM) abolishes the field potentials induced by LOT stimulation. The subsequent addition of 4AP to the perfusate has no effect on the evoked potentials. Partial recovery is observed upon washout.

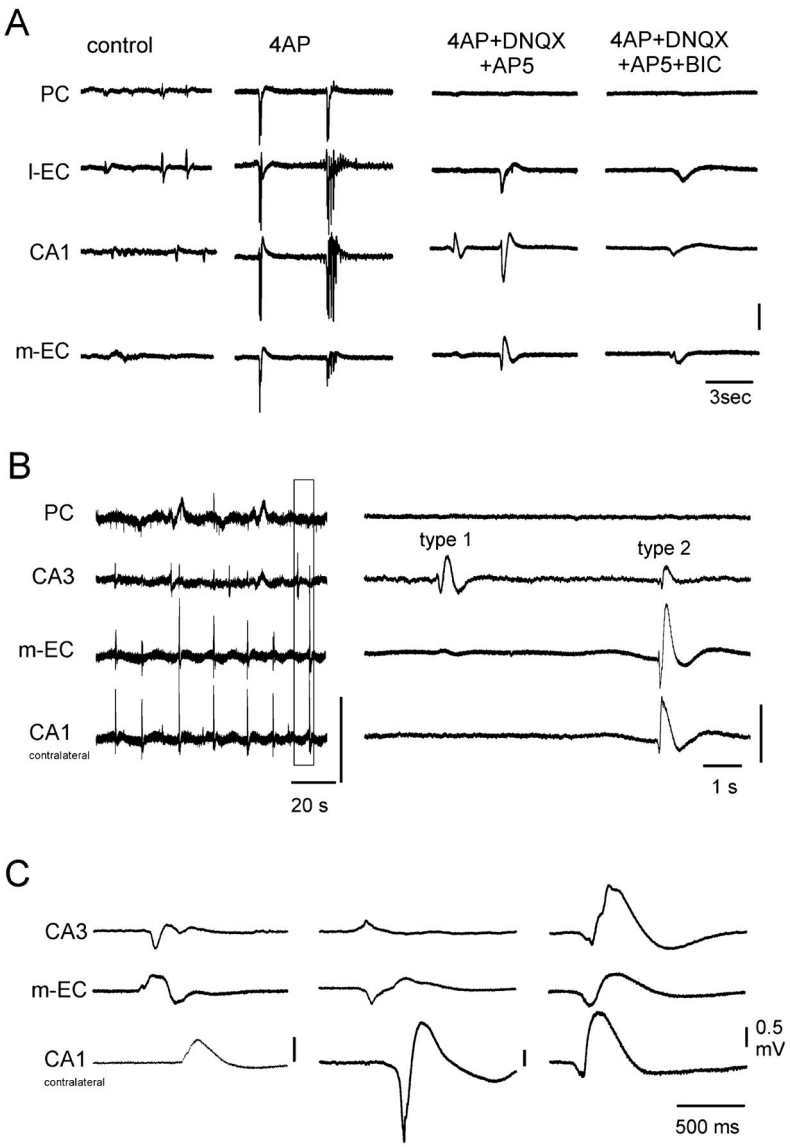

Fig. 5.

(A) Epileptiform activity induced by 4AP application in the PC, l-EC, CA1 and m-EC of the isolated brain preparation is abolished by DNQX and AP5. The application of these glutamatergic receptor antagonists reveals potentials in the EC / hippocampal region that are abolished by further administration of the $GABA_A$ receptor blocker bicuculline (BIC) (50 μM). (B) Spontaneous potentials recorded in the PC, CA3 and m-EC and in the CA1 of the contralateral hemisphere during 4AP, CNQX (50 μM) and AP5 (100 μM) perfusion. On the left, traces are presented with a slow time scale to highlight the periodicity of these field potentials. An expansion of the trace outlined by the dotted line is shown on the right. Note that type 1 potentials do not propagate outside the hippocampus, whereas type 2 activity propagates to CA3, m-EC and the contralateral CA1. (C) Examples of type 2 potentials that originate from and propagate to different structures.

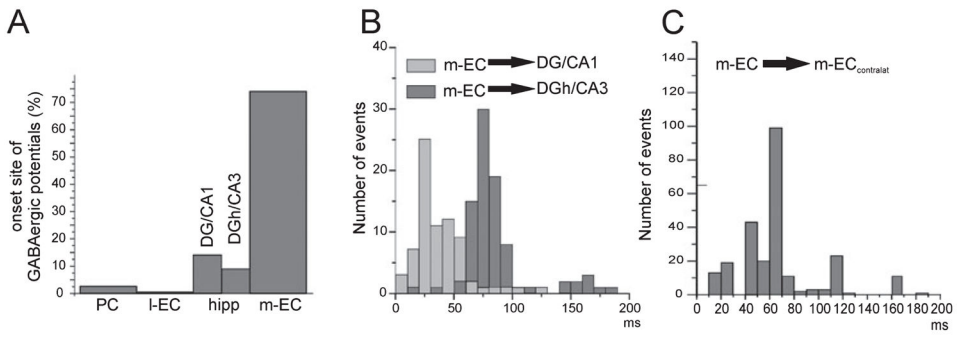

Fig. 6.

(A) Distribution histogram of the site of initiation of type 2 potential events in the PC, l-EC, hippocampus and m-EC. The hippocampus was subdivided into the DG / CA1 region and DG hilus (DGh) / CA3 region on the basis of the reconstructed position of the recording electrode. The analysis includes 528 events from nine experiments. (B) Distribution histogram of the onset delays of type 2 potentials originating in the m-EC and propagating to different portions of the hippocampus (DG / CA1 and DGh / CA3, respectively). (C) Distribution histogram of the onset delays of the type 2 potential originating in the m-EC and propagating to the contralateral m-EC.

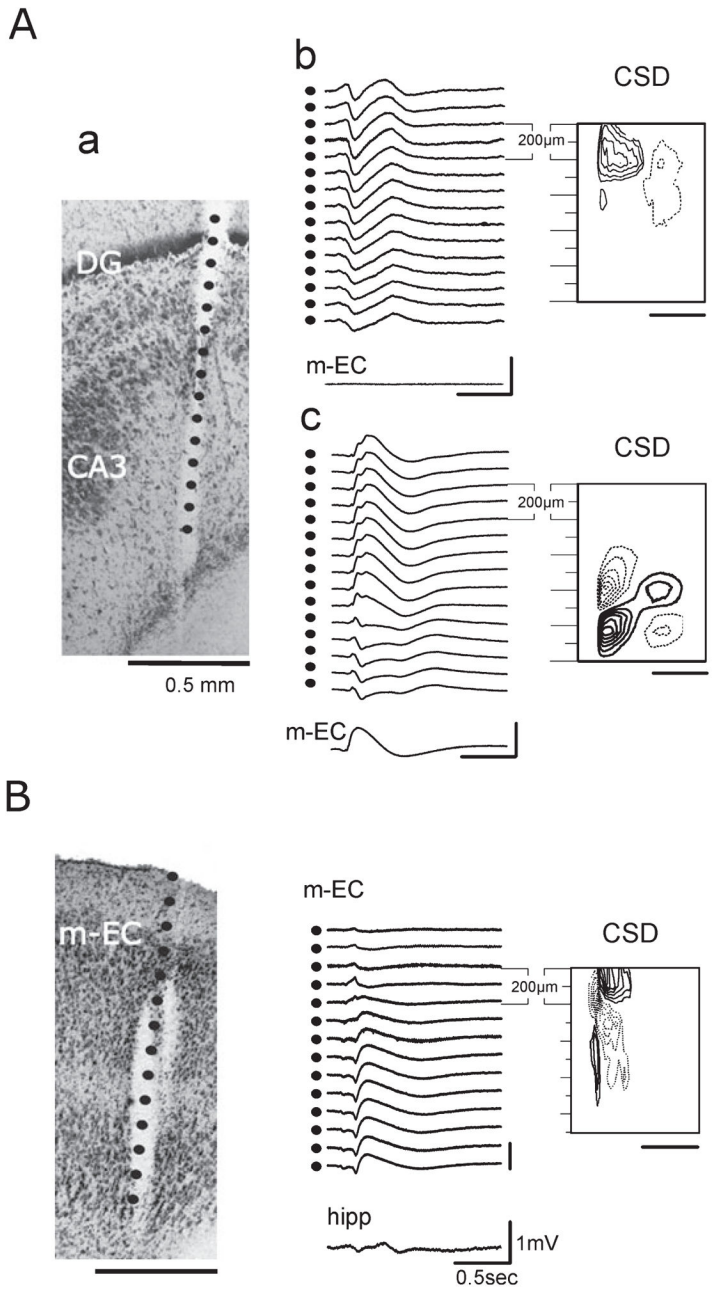

Fig. 7.

(A) Type 1 and type 2 potentials recorded from the same position with a recording silicon probe during one experiment. (a) The calculated position of the recording contacts is superimposed on the histological reconstruction of the track of the 16-channel silicon probe (100 μm separation between recording sites). Calibration bar: 500 μm. (b and c) Laminar profiles were recorded with the same probe position. (b) Field potential profile of type 1 potential recorded in the hilus of the DG as shown by the CSD contour plot (isocurrent lines at 0.01 mV / mm^2). No activity was recorded with a glass electrode positioned in the m-EC. (c) Type 2 potential recorded in the hippocampus; the simultaneous activity in the m-EC is

also illustrated. Corresponding CSD contour plot shows a local generation in CA3 (isocurrent lines at 0.05 mV / mm^2). (B) Type 2 potential recorded in the m-EC. On the left is shown the reconstruction of the position of the multichannel probe (100 μm between recording sites) on the histological section (calibration bar: 500 μm). Field potential profile of the type 2 potential recorded in the m-EC and the trace simultaneously recorded in the hippocampus showing the propagation of the potential (represented in the middle). On the right, the relative CSD contour plot (isocurrent lines at 0.02 mV / mm^2) shows an early sink in layer II–III (500–700 μm depth) followed by an associative sink in the superficial layers (0–200 μm depth).

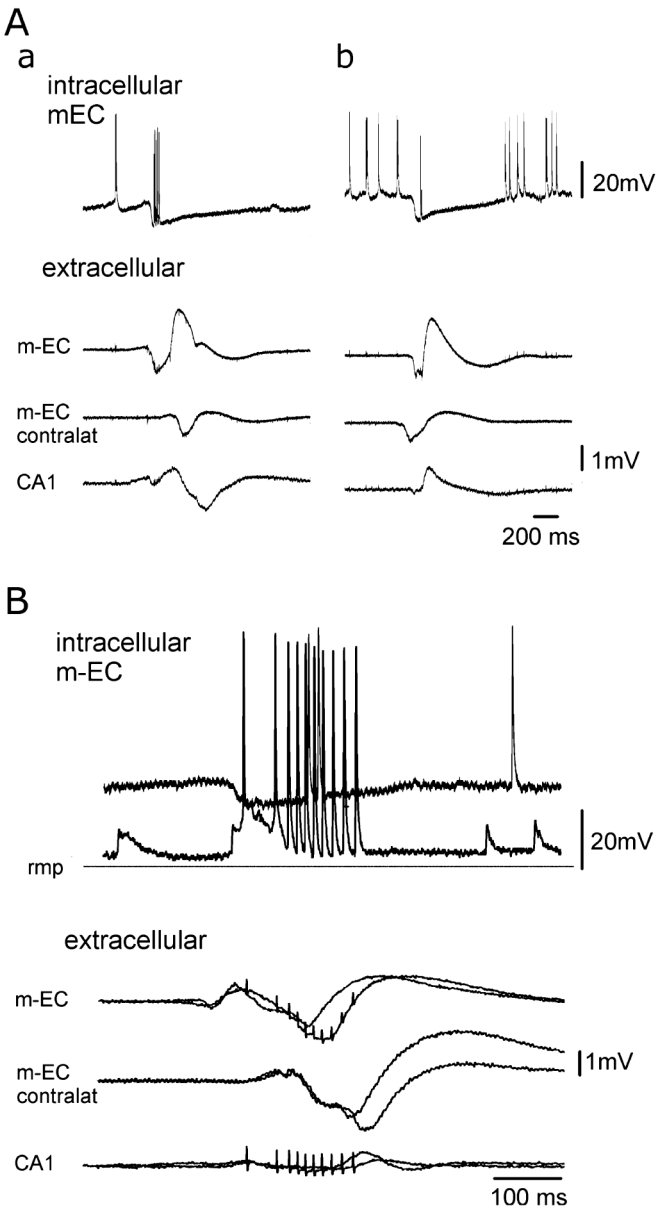

Fig. 8.

Intracellular recordings performed in the m-EC during $GABA_A$-receptor-mediated spontaneous interictal potentials obtained with the simultaneous perfusion of DNQX, AP5 and 4AP. (A) Intracellular (upper traces) and extracellular activities recorded in the m-EC ipsilateral and contralateral to the intracellular recording site and in ipsilateral CA1 during a type 2 potential that initiated in the m-EC (a) and during a GABAergic event that is propagated from the m-EC contralateral to the intracellular recording site (b). The two events were recorded from the same m-EC neuron located in layers II–III. The cell was depolarized to highlight the IPSP that correlates to the GABAergic potential. (B) Superimposed intracellular and extracellular activities recorded in the m-EC ipsilateral and contralateral to the intracellular recording side and in the ipsilateral CA1 during a type 2 GABAergic potential that initiates in the m-EC. The intracellular correlates of two identical

GABAergic potentials were recorded at different membrane polarizations during the injection of steady intracellular currents (resting membrane potential, −69 mV) to illustrate the IPSP reversal. Note that action potential firing interrupted the IPSP.